
Article:
Thompson, N.B.A., Middleburgh, S.C., Evitts, L.J. et al. (3 more authors) (2020) Short communication on further elucidating the structure of amorphous U2O7 by extended X-ray absorption spectroscopy and DFT simulations. Journal of Nuclear Materials, 542. 152476. ISSN 0022-3115

https://doi.org/10.1016/j.jnucmat.2020.152476

Title: Short Communication on Further Elucidating the Structure of Amorphous U_2O_7 by Extended X-ray Absorption Spectroscopy and DFT Simulations

Authors: Nathan B.A. Thompson[a], Simon C. Middleburgh[b], Lee J. Evitts[b], Matthew R. Gilbert[c], Martin C. Stennett[a], Neil C. Hyatt[a]

[a]University of Sheffield, Department of Materials Science and Engineering, Sir Robert Hadfield Building, Sheffield, UK, S1 3JD
[b]Nuclear Futures: Materials, Bangor University, Bangor LL57 1UT, UK
[c]AWE, Aldermaston, Reading, UK, RG7 4PR

*Corresponding author. Email addresses: nbathompson1@sheffield.ac.uk (N Thompson), s.middleburgh@bangor.ac.uk (S Middleburgh), l.evitts@bangor.ac.uk (L Evitts), matthew.gilbert@awe.co.uk (M Gilbert), m.c.stennett@sheffield.ac.uk (M Stennett), n.c.hyatt@sheffield.ac.uk (N Hyatt).

Keywords: U_2O_7, X-ray absorption, DFT, simulation, bonding.

Abstract:
The structure of amorphous U_2O_7 has been examined by extended x-ray absorption near edge spectroscopy (EXAFS) and modelled using density functional theory (DFT) simulations. A hybridised metastudtite-UO_3 structure is proposed, consisting of peroxide bonds ($O\text{-}O_{peroxo}$), uranyl units ($U{=}O_{yl}$) and U-O bonding. Experimental and simulated X-ray diffraction (XRD) is used to confirm the proposed structure.

1. Main Body:

At both the front and back-end of the nuclear fuel cycle, spent uranium may be reprocessed via calcination of a uranyl peroxide species to form uranium trioxide (UO_3), a compound commonly used in the storage of low enriched uranium waste.[1] The thermal decomposition of uranyl peroxide tetrahydrate, or studtite ($[(UO_2)(O_2)(H_2O)_2]\cdot 2H_2O$), undergoes four distinct stages; first dehydrating to uranyl peroxide dihydrate, or metastudtite ($[(UO_2)(O_2)(H_2O)_2]$), followed by further dehydration to an amorphous phase, thought to be stoichiometric U_2O_7, decomposing further to crystalline α-UO_3 and α-U_3O_8 at higher temperatures.

Very few studies have been carried out investigating U_2O_7 experimentally and theoretically, and given the existence of U_2O_7 as an intermediate in the thermal processing of uranyl peroxide to UO_3, there is a need to characterise its structure. There is a lack of consensus in the literature on a single structure or stoichiometry of the amorphous phase U_2O_7, which has been attributed to amorphous UO_{3+x} and hydrated species thereof.[2,3,4] A study by Odoh et al. in 2016, reported a structure for am-U_2O_7, obtained through density functional theory (DFT) and supported by neutron scattering experiments.[5] In 2019, Shields et al. applied DFT to a potentially stable crystalline U_2O_7 phase, to better understand the structure of the amorphous compound. They reported a structure comprising two distinct uranium sites, each six and eight-coordinate consisting of peroxide units and U-O bonds.[6] From mass loss previously determined by thermogravimetric analysis (TGA-MS), a stoichiometry of U_2O_7 has been calculated and applied to this study.[7] Here, we report analysis of U L_3 Extended X-ray Absorption Fine Structure, coupled with computational simulations, to provide further insight into the local structure of the amorphous U_2O_7 phase.

A single batch of uranyl peroxide tetrahydrate, or studtite ($[(UO_2)(O_2)(H_2O)_2]\cdot 2H_2O$), was heated (at pre-determined temperatures) to produce metastudtite (150 °C) and U_2O_7 (250, 350 and 450 °C) in an N_2 atmosphere at 10 °C/min. UO_3 was obtained by further heating to 535 °C, and U_3O_8 to 1050 °C, for comparison. A Netzsch TG 449 F3 Jupiter simultaneous thermal analyser was used to ensure accurate sample heating. X-ray absorption spectroscopy (XAS) data were acquired carried on beamline BL-27B, at The Photon Factory, High Energy Accelerator Research Organisation (KEK), Japan.[8] The obtained XAS data were analysed using the Demeter analysis package. Data normalisation was carried out using Athena, and fitting was performed in Artemis.[9] Artemis uses the FEFF code to perform *ab initio* multiple scattering calculations based on clusters of atoms generated from crystallographic information files (CIF). Further information on the data collection and analysis is supplied in the supplementary information.

U_2O_7 was modelled using the Vienna Ab-initio Software Package (VASP) version 5.4.4. 90 atoms were placed randomly within a cubic supercell of defined dimensions. Initial densities of 6.80 g/cm^3 and 1.60 g/cm^3 were trialled; while the former is the experimental density for this compound, it has previously been reported that lower densities, such as the latter, are required when modelling amorphous structures.[10-12] 20 different randomised structures were produced to ensure that the amorphous nature of the system is adequately captured.[12,13] Trials with 72-atom supercells were also carried out to understand the impact of system size on the final relaxed structure of the compound. Powder diffraction patterns and radial pair distribution functions were obtained using the Crystal Maker® CrystalDiffract 6 software. Further information on the simulation procedure and analysis is supplied in the supplementary information.

Information about the local structural environment around the uranium cations was obtained by analysis of the EXAFS region of the XAS data. A standard background subtraction and normalisation procedure was performed to the raw absorption data to generate normalised k^3-weighted spectra.[9,14] Applying a Fourier transform to the k^3-weighted EXAFS spectra produced a FT k^3 $|\chi(k)|$ or R-space transforms, where peaks represent the position of *shells* of atoms surrounding the central uranium absorber atom. The *shells* observed were not the result of a single uranium absorber neighbour interaction but were a combination of single and multiple scattering interactions. For metastudtite the first *shell* was situated at a distance of ca. 1.4 Å (un-corrected for phase shift) and a second was observed at ca. 1.8 Å. These *shells* correspond to contributions from the peroxide and uranyl scattering paths, respectively. These features became less well resolved in the heat treated samples consistent with the observed change in the structure and the contributing interatomic scattering paths (Supporting Information, Figure S1).

Given the X-ray amorphous nature of U_2O_7 no CIF exists, so scattering paths used in modelling the EXAFS data were generated from the crystalline metastudtite structure, which is the thermal precursor to the amorphous phase.[15] The generated paths are shown in Table 1, below. For each path, the path length (R) and the thermal parameter (σ^2) were calculated. The coordination number was determined and fixed for each path by first fitting the paths of the uranyl unit; the model was developed as a result of this successful fit.

	U_2O_7 (350 °C)	
Parameter		**Error (±)**
E_0 (eV)	6.0	2.8
R(U-O1) (Å)	1.86	0.01
N(U-O1)	1	*
R(U-O2) (Å)	1.80	0.01
N(U-O2)	1	*
σ^2(O1,O2) (Å^2)	0.004	0.001
R(U-U) (Å)	4.63	0.3
N(U-U)	2	*
σ^2(U) (Å^2)	0.026	0.06
R(U-O3) (Å)	2.52	0.04
N(U-O3)	2	*
σ^2(O3) (Å^2)	0.007	0.002
R(U-O4) (Å)	2.32	0.02
N(U-O4)	1	*
σ^2(O4) (Å^2)	0.003	*
R(U-O3-O3) (Å)	3.37	*
N(U-O3-O3)	2	*
σ^2(O3-O3) (Å^2)	0.014	*
R-factor	0.039	

Table 1: Scattering paths used to fit the U_2O_7 EXAFS data. All paths were generated by FEFF using a CIF for the metastudtite structure. Full fitting parameters and values are included in the Supplementary Information document (Table S3).

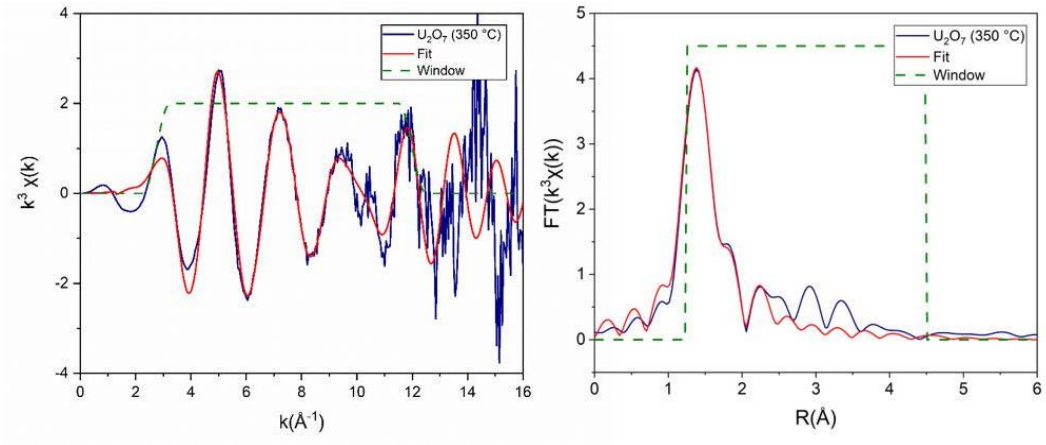

Figure 1: EXAFS spectra of metastudtite sample heated at 350 °C: Normalised k^3-weighted spectra (left) and Fourier transform of k^3-weighted spectra [FT $k^3X(k)$ (right).

The fit of the refined model to the data is shown in Figure 1. This model returned a satisfactory fit (R factor = 0.035) to the intense feature at ca. 1.4 Å and the shoulder at ca. 1.8 Å. The paths used in this fit suggest that U_2O_7 consists of a uranyl unit, UO_2^{2+}, similar to that found in metastudtite. Only one path generated by FEFF from the metastudtite structure, U-O2 O3-U, was excluded, which requires a linear uranyl species and hence a 90° angle with respect to oxygen co-ordinated in the equatorial

plane. Additionally, including a multiple scattering U- O1 U O2-U path with a 180 ° bond angle returned an unsatisfactory fit. As these paths did not fit the experimental data, U_2O_7 may instead contain a bent, rather than linear, uranyl bond. The compound possesses a peroxide unit, O-O, represented by O3 in the model. A fourth oxygen, O4, is also present, at a typical distance for a U-O bond. These results correspond well with the structure proposed by Odoh et al., despite their findings of slightly different bond lengths to those found in metastudtite.[5] The refined model was successfully fitted to each of the four samples within the U_2O_7 temperature range, suggesting that the local structure is not sensitive to thermal processing history. An attempt was made to fit the experimental data with the CIF proposed by Shields et al., from their two-site crystalline U_2O_7 model.[6] In spite of this model returning a fit with a low R-factor, it was rejected based on the generation of multiple negative thermal parameters; thus, the more likely atomic structure for amorphous U_2O_7 seems to be closer to that of metastudtite.

To improve understanding of the U_2O_7 structure on the atomic scale, DFT simulations were performed with 90 atoms, equivalent to 10 U_2O_7 units. After structural relaxation using an initial density of 6.80 gcm^{-3}, the final densities of the systems were significantly higher, averaging 11.55 gcm^{-3}. In addition, there was a notable absence of U-O uranyl bonds, 1.7 - 1.8 Å, in the RDF (Figure 2).[5,6,16]

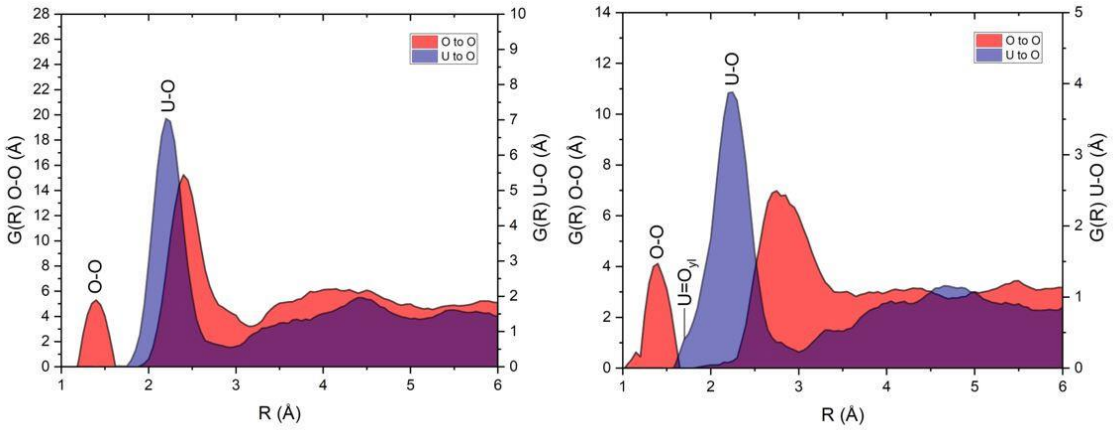

Figure 2: Average radial distribution function of simulated U_2O_7 models with 90 atoms at densities of 11.55 gcm^{-3} (left) and 7.40 gcm^{-3} (right).

Subsequently, simulations were carried out to equilibrate the local atomic structure, before full relaxation of these simulations at a significantly lower initial density (a = 18.369 Å, density of 1.60 gcm^{-3}) before full optimisation of the cell (allowing the cell size to equilibrate). This procedure returned a density closer to experimental observation, 7.40 gcm^{-3}, and a greater number of uranyl bonds in the final relaxed structure (Figure 2b).[10] There appeared to be, therefore, a negative correlation between the fully relaxed supercell density and propensity for uranyl bonding in this simulation study. This can be explained by the nature of the uranyl bonds observed in the simulated structures: the structure can be described as uranyl units with a variable degree of interconnection through shared equatorial oxygens, similar to the description of U_2O_7 by Odoh et al. The uranyl bonds are observed where the oxygen is non-bridging to another monomer unit – a more prevalent observation in the lower density, lower network connectivity structure.[17] As a result, only the results from the second method were taken forward for analysis.

Figure 3 shows a representative fully relaxed model of U_2O_7 obtained by DFT simulations. Figure 3a shows the bridging of two uranium atom sites via a shared peroxide ion, similar to that found in metastudtite. The U1 and U2 polyhedra are effectively 3 and 7 coordinate, respectively (Equations 1-

3 in the Supporting Documentation). U1 consists of two bent, axial uranyl bonded oxygen ions at a length of ~1.86 Å, while the remaining oxygen atoms are bonded in the typical U-O range between 2.1 – 2.5 Å. U2 consists only of oxygen atoms bonded within this range, suggesting no uranyl units are present on this site. However, both U1 and U2 are bonded to the peroxide oxygen atoms at a distance of approximately 2.4 Å; the O-O distance in the peroxide group is 1.47 Å.

Figure 3b, demonstrates the linking of three uranium atoms by a peroxide group and a single bridging oxygen atom. Similarly to U1, only U5, with an effective polyhedral coordination (SI, Eq. 1-3) of 3 contains a uranyl unit, while U3 and 4 (6 and 5 coordinate, respectively) consist only of U-O bonds. This is indicative of a correlation between the uranium coordination number and prevalence of uranyl species in U_2O_7.

Of particular interest was the retention of metastudtite features, such as peroxide and uranyl bonding, while other uranium sites were seemingly more akin to the bonding present in α-UO_3 (Figure 3c). Thus, these DFT simulations reveal that the structure of U_2O_7 consists of a widely disordered hybridised network of metastudtite-like and UO_3-like bonding, contributing to a bulk amorphous material.

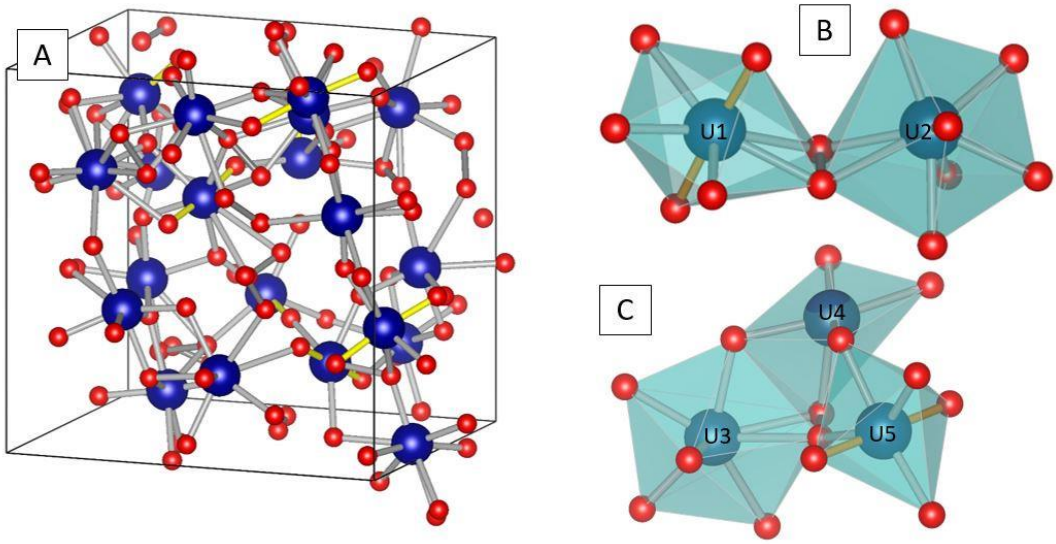

Figure 3: A representative, fully relaxed structure of U_2O_7 (in a box of sides a=9.63, b=11.45 and c=11.49 Å) from VASP DFT simulations (A), with reduced visualisations B and C (right). B exhibits metastudtite-like bonding and C, UO_3-like bonding. Uranyl bonds ($U=O_{yl}$) are shown in yellow.

The average RDF for these simulated models was somewhat in agreement with neutron scattering data provided in previous studies, as well as the EXAFS data presented in this work. The peak at ~ 1.4 Å corresponds to the $O\text{-}O_{peroxo}$ bond, while a small, broad shoulder peak beginning at ca. 1.8 Å is attributed to the uranyl $U=O_{yl}$ bond. The latter appears significantly lower in relative frequency than was found in previous studies, although contributes in part to the larger peak at ca. 2.3 Å, corresponding to U-O bonding. The prevalence of the U=Oyl bond can be used as a measure of the network connectivity of the amorphous structure, where increases in frequency suggest a less connected structure. Molecular order beyond this distance was lost in the U_2O_7 model.
An XRD pattern was simulated from the average of the 20 simulation runs, using X-rays of 1.541 Å wavelength and a Gaussian peak profile. The average simulated XRD plot for this model consisted of broad diffuse scattering at $2\theta \approx 26°$ and 47°, in agreement with experimental findings (Supporting Information, Figure S4). Also observed were diffuse scattering at $2\theta \approx 12°$ and 18°, also found in experimental results but at much lower intensity than in the simulated pattern.

From these EXAFS and DFT results, it can be concluded that the amorphous compound, U_2O_7, has a structure that contains features found in both metastudtite and α-UO_3. In EXAFS, the quality of the fit of the atomic metastudtite scattering paths to experimentally obtained U_2O_7 spectra suggests that the compound contains O-O_{peroxo}, U=O_{yl} and U-O bonds. This is supported by the DFT simulations, visualised as a relaxed structure of metastudtite and UO_3-like atomic environments. The relaxed simulated model has an average density of 7.40 gcm^{-3}, similar to the experimental density of 6.80 gcm^{-3} reported previously.[10] The higher density with respect to the experimental structure is a result of higher connectivity in the simulation cells, made apparent by the reduction in the expected concentration of U=Oyl bonds. Despite the higher density, the trends in the local structure were consistent with the experimental data, the average RDF for this model shows significant bonding at similar interatomic distances fitted in EXAFS. A simulated XRD pattern was obtained and corresponded well with experimentally obtained data, further suggesting that the simulated model reported here bears the experimental structure of U_2O_7, namely, a widely disordered hybridised network of metastudtite and UO_3-like bonding, contributing to a bulk amorphous material. Further work will be carried out to understand the role of residual hydrogen species in the structure and other impurities that may impact the network connectivity. This structure, according to fitting of the refined model to EXAFS data over the bounding temperature range (250 – 450 °C), is seemingly insensitive to thermal processing history.

Acknowledgements: This research utilised the HADES/MIDAS facility at the University of Sheffield established with financial support from EPSRC and BEIS, under grant EP/T011424/1.[18] SCM and LJE were supported Sêr Cymru II programmes funded through the Welsh European Funding Office (WEFO) under the European Development Fund (ERDF). Computing resources were made available by HPC Wales and Supercomputing Wales. Collection of the XAS data was performed under the approval of the Photon Factory Advisory Committee (Proposal No. 2017G187), with support from EPSRC under grant reference EP/P013600/1; the support of Yoshihiro Okamoto (JAEA) and Noriko Usami (KEK) during the experiment is gratefully acknowledged.

Funding: This work was supported by AWE Plc. through the University of Sheffield, as a part of the Next Generation Nuclear Centre for Doctoral Training consortium.

Data Availability Statement: The raw/processed data required to reproduce these findings cannot be shared at this time due to legal or ethical reasons, and as the data also forms part of an ongoing study.

References:

1. Pöyry Energy Ltd and Wood Nuclear Ltd, 2019 UK Radioactive Material Inventory, Department for Business, Energy & Industrial Strategy (BEIS) and the Nuclear Decommissioning Authority (NDA), 2019.
2. T. Sato, Uranium Peroxide Hydrates, Naturwissenschaften, 1961, 48, 668-668. doi: https://doi.org/10.1007/BF00592833.
3. X. Guo, D. Wu, H. Xu, P. Burns and A. Navrotsky, Thermodynamic studies of studtite thermal decomposition pathways via amorphous intermediates UO_3, U_2O_7, and UO_4, J. Nucl. Mater., 2016, 478, 158-163. https://doi.org/10.1016/j.jnucmat.2016.06.014.
4. R. Thomas, M. Rivenet, E. Berrier, I.de Waele, M. Arab, D. Amaraggi, B. Morel and F. Abraham, Thermal decomposition of $(UO_2)O_2(H_2O)_2{\cdot}2(H_2O)$: Influence on structure, microstructure and hydrofluorination, J. Nucl. Mater., 2017, 483, 149-157. Doi: https://10.1016/j.jnucmat.2016.11.009.

5. S. Odoh, J. Shamblin, C. Colla, S. Hickam, H. Lobeck, R. Lopez, T. Olds, J. Szymanowski, G. Sigmon, J. Neuefeind, W. Casey, M. Lang, L. Gagliardi and P. Burns, Structure and Reactivity of X-ray Amorphous Uranyl Peroxide, U_2O_7, J. Inorg. Chem., 2016, 55, pp.3541-3546. doi: https://doi.org/10.1021/acs.inorgchem.6b00017.
6. A. Shields, A. Miskowiec, J. Niedziela, M. Kirkegaard, K. Maheshwari, M. Ambrogio, R. Kapsimalis and B. Anderson, Shining a light on amorphous U2O7: A computational approach to understanding amorphous uranium materials, Opt. Mater., 2019, 89, 295-298. https://doi.org/10.1016/j.optmat.2019.01.040.
7. N. Thompson, Forensic signatures of nuclear materials processing. Cranfield Online Research Data (CORD), 2017. doi: https://doi.org/10.17862/cranfield.rd.5585398.v1
8. H. Konishi, A. Yokoya, H. Shiwaku, H. Motohashi, T. Makita, Y. Kashihara, S. Hashimoto, T. Harami, T.A. Sasaki, H. Maeta, H. Ohno, H. Maezawa, S. Asaoka, N. Kanaya, K. Ito, N. Usami, K. Kobayashi, Synchrotron radiation beamline to study radioactive materials at the Photon factory, Nucl. Instrum. Methods**,** A372, 322 (1996). doi: https://doi.org/10.1016/0168-9002(95)01241-9.
9. B. Ravel and M. Newville, ATHENA, ARTEMIS, HEPHAESTUS: data analysis for X-ray absorption spectroscopy using IFEFFIT, J. Synchrotron Radiat., **12**, 537–541 (2005). doi: https://10.1107/S0909049505012719.
10. L. Sweet, C. Henager, S. Hu, T. Johnson, D. Meier, S. Peper and J. Schwantes, PNNL-20951: Investigation of Uranium Polymorphs, PNNL for U.S Department of Energy, 2011. doi: https://10.13140/RG.2.1.3073.0004.
11. G. Kresse and J. Hafner, Ab initio molecular dynamics for liquid metals, Phys. Rev. B, 1993, 47, 558.
12. D. King, S. Middleburgh, A. Liu, H. Tahini, G. Lumpkin, M. Cortie, Formation and structure of V-Zr amorphous alloy thin films, Acta Mater., 2015, 83, 269-275. doi: https://10.1016/j.actamat.2014.10.016.
13. M. Rushton, I. Ipatova, L. Evitts, W. Lee, S. Middleburgh, Stoichiometry deviation in amorphous zirconium dioxide, RSC Adv. 9 (29), 2019, 16320-16327. doi: https://doi.org/10.1039/C9RA01865D.
14. M. Newville, IFEFFIT: interactive XAFS analysis and FEFF fitting, Journal of Synchrotron Radiation, 8 (2001) 322-324. doi: https://doi.org/10.1107/S0909049500016964.
15. P. Weck, E. Kim, C. Jové-Colón and D. Sassani, Structures of uranyl peroxide hydrates: a first-principles study of studtite and metastudtite, Dalton Transactions, 2012, 41, 9748. doi: https://doi.org/10.1039/C2DT31242E.
16. P. Burns and K. Hughes, Studtite, $[(UO_2)(O_2)(H_2O)_2](H_2O)_2$: The first structure of a peroxide mineral, Am. Mineral., 2003, 88, 1165-1168. doi: http://10.2138/am-2003-0725.
17. R. Hill, D. Brauer, J. Non-Cryst. Solids, 2011, 357, 24, 3884-3887. doi: https://doi.org/10.1016/j.jnoncrysol.2011.07.025.
18. N. C. Hyatt, C. L. Corkhill, M. C. Stennett, R. J. Hand, L. J. Gardner and C. L. Thorpe, IOP Conf. Ser. Mater. Sci. Eng., 2020, 818, 012022. doi: https://10.1088/1757-899X/818/1/012022.